Journal of Alloys and Compounds 508 (2010) 536–539

Contents lists available at ScienceDirect

Journal of Alloys and Compounds

journal homepage: www.elsevier.com/locate/jallcom

Preparation of heterostructured Ag/BaTiO$_3$ nanofibers via electrospinning

Heping Li, Yao sun, Wei zhang, Wei Pan*

State Key Laboratory of New Ceramic and Fine Processing, Department of Materials Science and Engineering, Tsinghua University, Beijing 100084, PR China

ARTICLE INFO

Article history:
Received 14 May 2010
Received in revised form 25 August 2010
Accepted 25 August 2010
Available online 21 September 2010

Keywords:
Heterojunctions
Composite materials
Ceramics
Nanofabrications
Electronic properties

ABSTRACT

Unique Ag/BaTiO$_3$ heterostructured nanofibers with a diameter of about 100 nm and coupled Ag nano-particles in the size range from several to 15 nm have been successfully fabricated by a facile electrospinning method. It was found that small and homogeneously distributed Ag nano-particles could decrease the crystallization temperature of BaTiO$_3$ nanofibers to a much lower value compared with bulk BaTiO$_3$ ceramics. The mechanism of the effect of Ag addition on BaTiO$_3$ crystallization is accordingly analyzed and discussed. Besides, *I–V* curve of Ag/BaTiO$_3$ nanofibers was also measured. The addition of Ag sharply increases the conductivity of BaTiO$_3$ nanofiber. The results may be benefit for the future study of one-dimensional heterostructured dielectric nano-materials.

1. Introduction

Heterostructured one-dimensional nano-materials, which exhibit enhanced properties in nanoelectronics, nanophotonics, sensing and catalysis, have been attracting notable attention in recent years [1–4]. Many methods could be adopted for preparing heterostructured nanofibers including thermal evaporation method [5], electrochemical deposition (ECD) [6], hydrothermal [7], vapor–liquid–solid epitaxy (VLS) [8], chemical vapor deposition, etc. Electrospinning is one of the newly developed methods for synthesis nanofibers due to its low cost and facile process [9]. Some work has recently been performed to fabricate novel heterojunction nanofibers with unique applications by electrospinning. Lin et al. have succeeded in preparation of electrospun Ag-ZnO nanowires exhibiting both excellent UV photoresponse [10] and photocatalytic activity [11]. Liu et al. have reported on the synthesis and assembly of ZnO/SnO$_2$ composite nanofibers via electrospinning, which showed higher photocatalytic activity than pure ZnO and SnO$_2$ nanofibers [12]. Liu and Sun have claimed that an efficient bicomponent TiO$_2$/SnO$_2$ nanofiber photocatalyst was fabricated by electrospinning [13]. More recently, the electrospun TiO$_2$/SnO$_2$ heterostructured nanofiber with a nano-necklace structure has been found to be an excellent photocatalyst with much higher photocatalytic activity than pure anatase nanofiber [14].

Barium titanate is a lead-free ferroelectric and piezoelectric material with a perovskite structure. The material owns high dielectric permittivity and has been extensively studied owing to its wide applications such as capacitors and nonvolatile ferroelectric random access memories [15]. Extraordinarily high dielectric constant has been found in new BaTiO$_3$-Ni hybrids prepared by a wet processing route [16]. However, there are few reports on the fabrication of one-dimensional BaTiO$_3$ based heterostructures.

In this letter, we report a newly electrospinning method for synthesis heterostructured Ag/BaTiO$_3$ nanofibers and their crystallization behavior with different Ag additions. The mechanism of effect of Ag addition on BaTiO$_3$ crystallization is accordingly discussed.

2. Experimental details

Using the typical electrospinning process, barium acetate, tetrabutyl titanate and silver nitrate were used as the starting materials. The precursor solution was prepared by dissolving tetrabutyl tatanate in the ethanol-acetic acid mixture (3.3:1, volume rate), stirring for 30 min to achieve complete mixing. While maintaining a 1:1 molar ratio of barium acetate and tetrabutyl tatanate, the mixture solution of barium acetate and silver nitrate was added into the tetrabutyl titanate solution, stirring at room temperature for 2 h to form homogeneous solution. Then, polyvinylpyrrolidone (PVP, MW = 1 300 000, Alfa Co.) was dissolved in the mixture in advance with a weight ratio of 1/13, and vigorously stirred for 3 h. The Ag contents in BaTiO$_3$ nanofibers were adjusted to be 0, 5.0, 11.0, 17.0 and 24.0 at.% respectively. After dissolution of all the compounds, Ag/BaTiO$_3$ composite nanofibers were electrospun by a typical setup of electrospinning expressed in the former research [17]. Using a peristaltic pump, the precursor solution was delivered to a needle made of stainless steel at a constant flow rate of 1.0 mL/h. The needle was connected to a high-voltage power supply. At an applied high voltage of 20 kV, a fluid jet was ejected from the needle. With the solvent evaporated, a charged fiber was collected on a grounded aluminum foil at an electrode distance of 20 cm.

Thermo-analysis (TG/DSC, STA 409, German) was conducted to determine the reaction process of the formation of Ag/BaTiO$_3$ nanofibers in air. The crystal structure and morphology of composite nanofibers were investigated by X-ray diffraction (XRD, D/max-2550, Rigaku Co., Tokyo, Japan), scanning electron microscopy

---

* Corresponding author. Tel.: +86 10 627 72858; fax: +86 10 627 71160.
E-mail address: panw@mail.tsinghua.edu.cn (W. Pan).

0925-8388/$ – see front matter © 2010 Elsevier B.V. All rights reserved.
doi:10.1016/j.jallcom.2010.08.114

(SEM, LEO-1530, Carl Ziess Co., Oberkochen, Germany) and transmission electron microscopy (HRTEM-2010F JEOL, Tokyo, Japan).

3. Results and discussion

Fig. 1 shows the SEM image of the Ag/$BaTiO_3$ nanofibers with diameters of about 100 nm. It can be seen that the fibers are uniform and the surface is quite smooth.

In the precursor nanofibers, most of the organic belonged to PVP. And from our previous study, PVP burnout and decomposition of organic groups are accomplished at a temperature of around 450°C [18]. So the composite nanofibers were firstly subjected to pyrolysis at 500 °C. Fig. 2(A) shows XRD spectras of Ag/$BaTiO_3$ composite nanofibers with different Ag contents calcined at 500 °C for 1 h with a heating rate of 10 °C min^{-1}. After calcination at 500 °C, the nanofibers with Ag at.% = 0 at.% are mainly amorphous. While with Ag content increasing to 5.0 at.%, the peaks of Ag and $BaTiO_3$ appears, indicating the formation of their recipient lattices. These peaks become more distinct when the Ag content goes up to 17.0 and 24.0 at.%, suggesting the development of a more integral lattice with more Ag addition. For the same specimen, the higher the calcination temperature is, the better the $BaTiO_3$ crystallized, as shown in Fig. 2(B). Thus, the addition of Ag into the $BaTiO_3$ nanofibers may decrease the crystallization temperature of $BaTiO_3$, which is identified by the XRD patterns of Ag/$BaTiO_3$ nanofibers with dif-

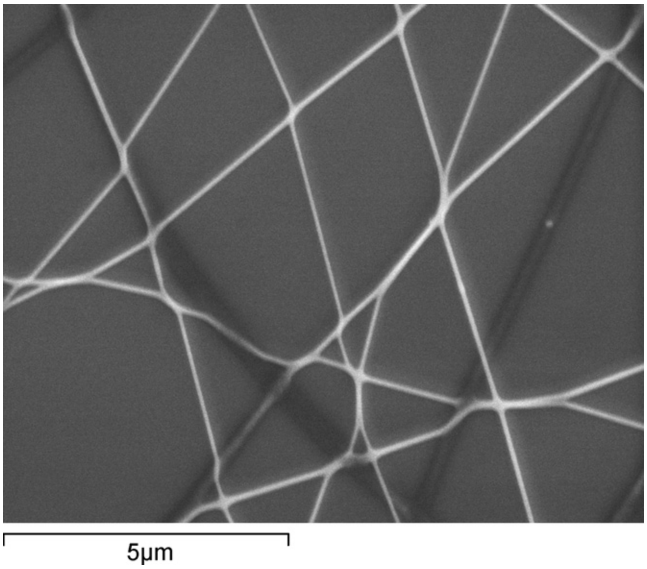

Fig. 1. Scanning electron microscope images of Ag/$BaTiO_3$ nanofibers with 5.0 at.% Ag calcined at 560 °C for 1 h.

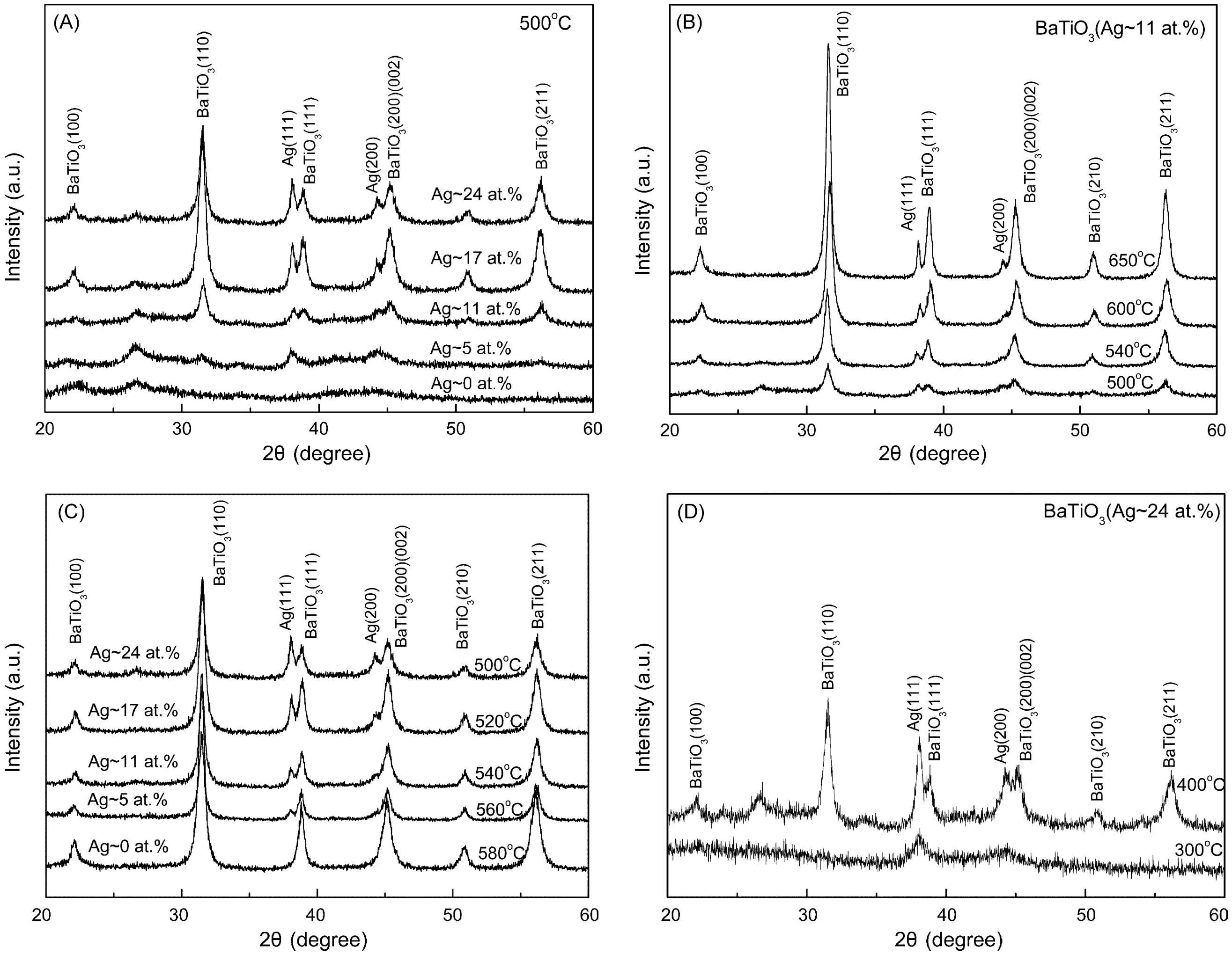

Fig. 2. XRD of Ag/$BaTiO_3$ nanofibers with corresponding Miller indices of Ag and $BaTiO_3$: (A) nanofibers with different Ag contents calcined at 500 °C for 1 h; (B) nanofibers with Ag at.% = 11.0 at.% calcined at different temperatures; (C) nanofibers with different Ag contents calcined at different temperatures for 1 h; (D) nanofibers with Ag at.% = 24.0 at.% calcined at 300 °C and 400 °C for 1 h.

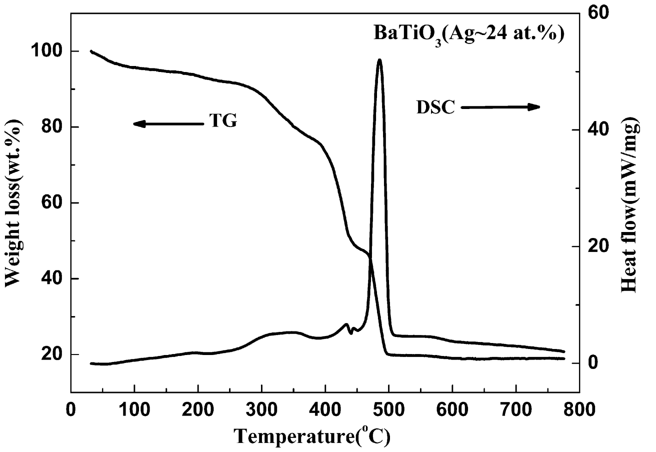

Fig. 3. Typical TG-differential scanning calorimetry curves of the non-woven mat of the composite nanofibers with Ag ~24 at.%.

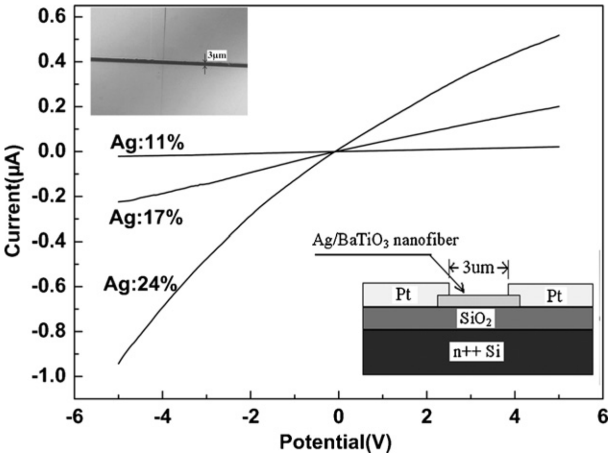

Fig. 5. (*I–V*) Measurement of Ag/BaTiO$_3$ nanofibers with different Ag contents calcined at 580 °C. Upper inset: Metallographic microscope image of the nanofiber across the Pt electrodes. Bottom inset: Schematic of device testing for Ag/BaTiO$_3$ nanofibers connecting two Pt electrodes with 3 um channel spacing.

ferent Ag contents calcined at different temperatures, shown in Fig. 2(C).

From the XRD results, even though the calcination temperature decreased with the Ag content increasing, the half-peak breadth of the specimens at 31.5° are all about 0.5 degree and accordingly the grain size of BaTiO$_3$ is calculated as 15–17 nm by Scherrer equation $L = 0.89\lambda/(\beta\cos\theta)$. Fig. 2(D) also shows that the Ag particle appeared at 300 °C indicated that the crystallization temperature of Ag is not higher than 300 °C in this case. From our previous study, it is known that the pure BaTiO$_3$ nanofibers are crystallized above 580 °C [19]. However, with the Ag content increasing from 0 at.% to 24.0 at.%, the crystallization temperature decreases from 580 °C to 400 °C, about 900 °C lower than that of the original crystallization temperature of barium titanate ceramics obtained by other methods. Moreover, from the calculation of the XRD results, no changing of the crystal constant of BaTiO$_3$ can be found, which suggests that there is no Ag doped into the crystal lattice of BaTiO$_3$. All XRD peaks are identified as Ag and BaTiO$_3$ peaks while no peaks of secondary phases or unwanted reaction phase have been observed, that means no reactions occurred during the heterostructured nanofiber's processing.

Thermo-analysis (TG/DSC) was conducted to determine the heat-treatment parameters, and the results are shown in Fig. 3. Below 250 °C, the weight loss is due to the evaporation of the volatile solvent, and that between 250 °C and 375 °C corresponds to the precipitation of Ag, which is approved by Fig. 2(D) with the peaks of Ag appearing at 300 °C. The exothermic DSC peaks at the temperature between 390 °C and 455 °C are considered to be the formation of perovskite structure BaTiO$_3$ due to the crystallization of the composite nanofibers shown in Fig. 2(D) with the appearance of the BaTiO$_3$ peaks at 400 °C. And the one at the temperature of about 480 °C is consistent with the PVP burnout. Above 500 °C, weight loss levels off and the pyrolysis is considered to be almost complete, indicating the formation of the pure BaTiO$_3$/Ag nanofibers.

How can the homogeneously distributed Ag have such a strong influence on the crystallization temperature of the BaTiO$_3$ nanofibers? This can be explained by the basic mechanism of the heterogeneous nucleation. When the precursor nanofibers were annealed at 300 °C, the Ag particles precipitate firstly in the Ag/BaTiO$_3$ nanofibers, indicated by Fig. 2(D). And in the case of ZnO/Ag, reported by Lin et al. [11], Fig. 4(A) clearly shows a homogeneous dispersion of silver nano-particles with sizes from several to 15 nm (dark spherical region) in the composite nanofibers. And Fig. 4(B) shows EDS spectrums of corresponding area in the nanofiber.

As a result, the precipitated Ag particles from the precursor nanofibers at lower temperature act as the nucleus of heterogeneous nucleation that can enhance the crystallization of BaTiO$_3$ in the nanofibers. As we know, it has been proved by both theories and experiments that large under-cooling is required by homogeneous nucleation. However, the existence of Ag particles could provide the nucleation interface and decrease the surface energy of crystal nucleus. In this case, the reduction of nucleation energy thus accel-

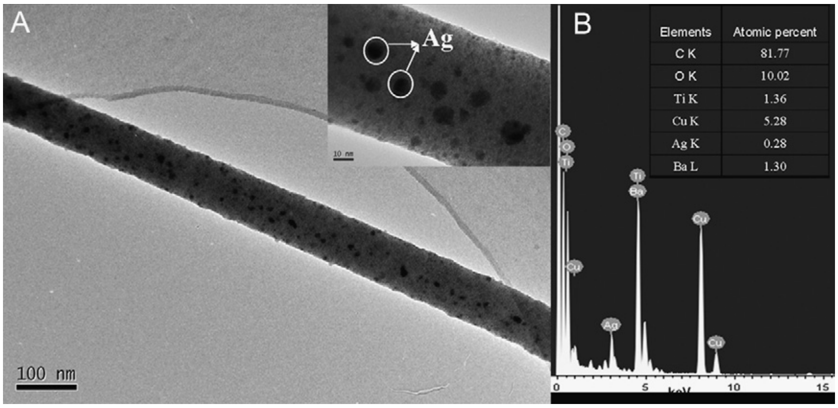

Elements	Atomic percent
C K	81.77
O K	10.02
Ti K	1.36
Cu K	5.28
Ag K	0.28
Ba L	1.30

Fig. 4. (A) TEM of Ag/BaTiO$_3$ nanofibers with Ag at.% = 24.0 at.% calcined at 300 °C for 1 h: right upper insert show more detailed micro-structure of the nanofiber by TEM; (B) EDS spectrums of corresponding area in the nanofiber.

erates the speed of crystallization of $BaTiO_3$ nanofibers and reduces the calcination temperature.

For electrical characteristics, single Ag/$BaTiO_3$ nanofiber bridging two electrodes was fabricated by modifying the layout of a collector, which is possible to assemble the thin fibers as uniaxially aligned arrays [20]. Then the nanofiber shown in Fig. 5 (upper inset) was severed using the probe tip of a Keithley probe station. Even though insulated composition ($BaTiO_3$) was introduced into the fiber system, Fig. 5 shows clear evidence that the *I*–*V* curve of this nanofiber was ohmic at room temperature. In the nanofibers, the nanosized Ag particles formed an interconnected network, through which the electric current was conducted. Therefore, the conductivity of Ag/$BaTiO_3$ nanofiber is increasing along with the Ag content.

4. Conclusions

A new heterostructured Ag/$BaTiO_3$ nanofibers with low-temperature crystallization has been successfully prepared by electrospinning. The distribution of Ag nano-particles is believed to significantly decrease the crystallization temperature of $BaTiO_3$ nanofibers. It is found that, with 24.0 at.% Ag addition, the $BaTiO_3$ nanofibers even crystallized at 400 °C. The reduction of the crystallization temperature is explained by the mechanism of heterogeneous nucleation and the addition of Ag sharply increases the conductivity of $BaTiO_3$ nanofiber. These results may be benefit for the future preparation of microcapacitor based on nano dielectric structures.

Acknowledgement

This work was supported by grant no. 50872063 from the National Natural Science Foundation of China.

References

[1] H.W. Kim, H.S. Kim, H.G. Na, J.C. Yang, C. Lee, J. Alloys Compd. 500 (2010) 175–180.
[2] L.Q. Qian, S.L. Wang, X. Jia, Y.Y. Liu, W.H. Tang, J. Alloys Compd. 477 (2009) 888–891.
[3] M. Lei, L.Q. Qian, Q.R. Hu, S.L. Wang, W.H. Tang, J. Alloys Compd. 487 (2009) 568–571.
[4] X.H. Huang, Y.W. Yang, X.C. Dou, Y.G. Zhu, G.H. Li, J. Alloys Compd. 461 (2008) 427–431.
[5] Y.X. Du, P. Ding, J. Alloys Compd. (2010), doi:10.1016/j.jallcom.2010.07.201.
[6] H. Asýl, Gür Emre, K. Çýnar, Appl. Phys. Lett. 94 (2009) 253501–253503.
[7] S.Y. Liu, T. Chen, X.P. Qu, J. Appl. Phys. 105 (2009) 114504–114508.
[8] S.P. Mondal, S.K. Ray, Appl. Phys. Lett. 94 (2009) 223119–223121.
[9] J. Li, E.H. Liu, W. Li, X.Y. Meng, S.T. Tan, J. Alloys Compd. 478 (2009) 371–374.
[10] D.D. Lin, H. Wu, W. Zhang, H.P. Li, W. Pan, Appl. Phys. Lett. 94 (2009), 172103(1-3).
[11] D.D. Lin, H. Wu, R. Zhang, W. Pan, Chem. Mater. 21 (2009) 3479–3484.
[12] R.L. Liu, Y.X. Huang, A.H. Xiao, H.Q. Liu, J. Alloys Compd. 503 (2010) 103–110.
[13] Z.Y. Liu, D.D. Sun, P. Guo, Nano. Lett. 7 (2007) 1081–1085.
[14] R. Zhang, H. Wu, D.D. Lin, W. Pan, J. Am. Ceram. Soc. 92 (2009) 2463–2466.
[15] S.O. Brien, L. Brus, C.B. Murray, J. Am. Chem. Soc. 123 (2001) 12085–12086.
[16] C. Pecharromμn, F. Esteban-BetegÛn, Adv. Mater. 13 (2001) 1541–1544.
[17] H. Wu, W. Pan, J. Am. Ceram. Soc. 82 (2006) 699–701.
[18] D.D. Lin, H. Wu, W. Pan, J. Am. Ceram. Soc. 90 (2007) 3664–3666.
[19] H.P. Li, H. Wu, W. Pan, J. Am. Ceram. Soc. 92 (2009) 2162–2164.
[20] D. Li, Y.L. Wang, Y.N. Xia, Nano. Lett. 3 (2003) 1167–1171.